Proceedings of the Institute of Acoustics

INFLUENCE OF PORE WALL ROUGHNESS ON SOUND ABSORPTION

K Attenborough
School of Engineering and Innovation, The Open University, Milton Keynes, UK

1 INTRODUCTION

According to a classical analytical theory, a 3 cm hard backed layer of a rigid solid matrix containing parallel identical narrow slits inclined to the surface normal with widths on the order of microns and separated by similarly narrow walls should provide useful broadband absorption[1,2,3]. Although, eventually, such porous structures might be created using additive manufacture, at present, 3D printing technology is not able to produce sufficiently narrow slits and separating walls. To test the theory, and, while doing so, to investigate the limitations of current technology, 3D printing has been used to manufacture cylindrical samples containing 0.3 mm wide, parallel, identical, vertical or zigzag slits separated by 0.4 mm in a rigid solid resin matrix[4]. Their normal incidence absorption coefficient spectra have been measured in an impedance tube. The zigzag configuration overcomes the difficulty of ensuring that inclined slits in a confined space are completely accessible to incident sound waves. Comparisons between measurements and predictions reveal discrepancies, especially for samples made by Fused Deposition Modelling (FDM)[4]. These discrepancies are attributed to rough internal surfaces and uneven slit cross sections perpendicular to the printing direction[4]. In this paper, a theory for sound absorption by a hard backed rigid solid layer containing parallel identical slits with sinusoidal cross sections is outlined and used to confirm that pore wall roughness is a feasible contributor to the differences between predictions and data for 3D printed samples.

There is increasing interest in the manufacture of sound absorbers from natural sources. The normal incidence sound absorption spectra of cylindrical porous samples made from crushed walnut shells and wood chips held together with an environmentally friendly binder have been measured. Since the surfaces of the shell fragments and wood chips used to make the samples are rough, they result in pores with rough walls. The sinusoidal slit theory is used to estimate the influence of pore wall roughness on their sound absorption.

Finally, the theory is used to illustrate the extent to which the deliberate introduction of sinusoidal slit cross sections could improve the sound absorption of a low flow resistivity hard backed rigid solid layer containing identical slits.

2 THEORY FOR SINUSOIDAL ROUGHNESS

A theory, developed initially for microperforated plates[5], can be extended to predict sound absorption by a material with a microstructure of parallel, identical, inclined slits with sinusoidal cross sections. Figure 1 (a) shows a single slit with mean width $2b$. The sinusoidal variation in the cross section has amplitude a and wavelength X. Figure 1(b) shows an array of such slits arranged vertically in a solid matrix to form a hard backed porous layer with a thickness d corresponding to N wavelengths of the sinusoidal cross section, i.e. $X = d/N$.

If $a/b \ll 1$ and $X \gg a$, the tortuosity T_r of a slit with mean semi width b having a sinusoidal cross section with amplitude a and wavelength X is given by[5]

$$T_r(a,X) = 1 + \left[\frac{e^{\frac{4\pi b}{X}}-1}{e^{\frac{4\pi b}{X}}+1}\right]\left(\frac{\pi a^2}{Xb}\right). \quad (1)$$

The flow resistivity of a slit of semi width b with parallel walls is $\left(\frac{3\mu}{b^2}\right)$, where μ is the dynamic viscosity of air. If the slit has the sinusoidal cross section shown in Figure 1(a), then the flow resistivity is increased by a factor S given by[5]

$$S(a,b,X) = \left\{\left[\frac{\left(2\left(\frac{a}{2b}\right)^2+1\right)}{\left(1-4\left(\frac{a}{2b}\right)^2\right)^{2.5}} - \frac{1}{\left(1-\frac{a}{b}\right)^3}\right]\left[\frac{2e^{-\frac{4b}{5X}}}{1+e^{-\frac{4b}{5X}}}\right] + \frac{1}{\left(1-\frac{a}{b}\right)^3}\right\} \quad (2)$$

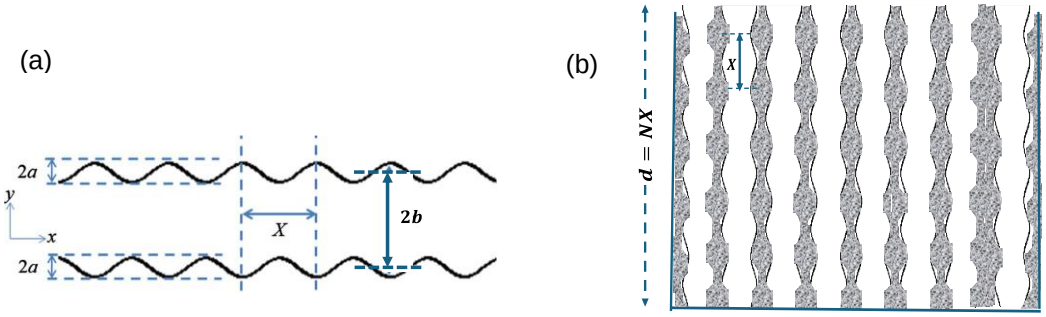

Figure 1. (a) A slit of mean width $2b$ and cross section varying sinusoidally with amplitude a and wavelength X,
(b) a porous hard backed layer of thickness d containing vertical identical slits each of which has the Fig.1(a) sinusoidal cross section and extends for N wavelengths ($d = NX$).

If the slits are inclined at an angle θ to the normal to the surface, then the tortuosity and flow resistivity are increased by a further factor T_θ given by[1]

$$T_\theta = 1/(\cos\theta)^2 \ . \quad (3)$$

The flow resistivity of a medium of bulk porosity Ω containing identical inclined slits, with the sinusoidal cross section shown in Fig.1(a), is given by[1,5]

$$R_S = \left(\frac{3\mu}{\Omega b^2}\right) T_r(a,X) T_\theta S(a,b,X) \quad (4)$$

According to Stinson[6], the complex density and complex compressibility of air in a parallel sided slit, are written as:

$$\rho(\omega) = \rho_0/H(\lambda),\ H(\lambda) = 1 - \tanh\left[\lambda\sqrt{(-i)}\right]/\lambda\sqrt{(-i)} \quad (5a,b)$$

$$C(\omega) = (\gamma P_0)^{-1}\left[\gamma - (\gamma-1)H\left(\lambda\sqrt{N_{Pr}}\right)\right] \quad (6)$$

where time dependence $e^{-i\omega t}$ is understood, $i = \sqrt{(-1)}$, ω is the angular frequency, $(\gamma P_0)^{-1} = (\rho_0 {c_0}^2)^{-1}$ is the adiabatic compressibility of air. γ, P_0, ρ_0, c_0 and N_{pr} denote the specific heat ratio of air, atmospheric pressure, air density, adiabatic sound speed and Prandtl number for air respectively. The dimensionless parameter $\lambda = b\sqrt{\omega/\nu}$, where $\nu = \mu/\rho_0$, μ being the dynamic coefficient of viscosity and b is the semi-width of the slit.

The bulk complex density ($\rho(\omega)$) and complex compressibility ($C(\omega)$) for a medium of porosity Ω containing identical, parallel, inclined, slits with sinusoidal cross sections are calculated from those for individual slits using Equations (1), (4), (7a) and (7b):

$$\rho_b(\omega) = (T_r T_\theta/\Omega)\rho(\omega),\ C_b(\omega) = \Omega C(\omega) \quad (7a,b)$$

The bulk propagation constant ($k(\omega)$) and relative characteristic impedance ($Z_C(\omega)$) of a porous material in which the pores are slits with sinusoidal cross sections of mean width $2b$ and with edge-to-edge separation $b(1-\Omega)/\Omega$ are calculated from Equations (7a), (7b), (8a) and (8b).

$$k(\omega) = \omega\sqrt{\rho_b(\omega)\, C_b(\omega)}\ ,\ Z_C(\omega) = (\rho_0 c_0)^{-1}\sqrt{\rho_b(\omega)/C_b(\omega)} \qquad (8a,b)$$

The surface impedance of a hard-backed porous layer of thickness *d* is:

$$Z(d) = Z_C(\omega)\coth(-ik(\omega)d) \qquad (9)$$

The plane wave reflection coefficient, *R*(*d*), and normal incidence absorption coefficient, $\alpha(d)$, for a hard-backed porous layer are given by Equations (10a), and (10b), respectively:

$$R(d) = \frac{\rho_0 c_0 - Z(d)}{\rho_0 c_0 + Z(d)}\ ,\ \alpha(d) = 1 - \left|\left(R(d)\right)^2\right|. \qquad (10a,b)$$

3 ABSORPTION BY 3D PRINTED SAMPLES

Opiela *et al*[4] have made impedance tube measurements of the normal incidence absorption spectra for 49.5 mm thick samples containing 0.3 mm wide parallel slits which are either vertical or with 45° zigzags. The slit separation of 0.4 mm corresponds to a porosity of 0.43. Figure 2 (Figure 8 from Ref.4) shows the measured and predicted for vertical slits. The predictions were obtained both analytically and numerically, the latter by using a Finite Element code. Although the predictions agree with each other, they depart from the data between the quarter wavelength resonances, where the measured absorption is higher than predicted. Also, the second quarter wavelength resonance in the measured spectrum is slightly lower in frequency than predicted.

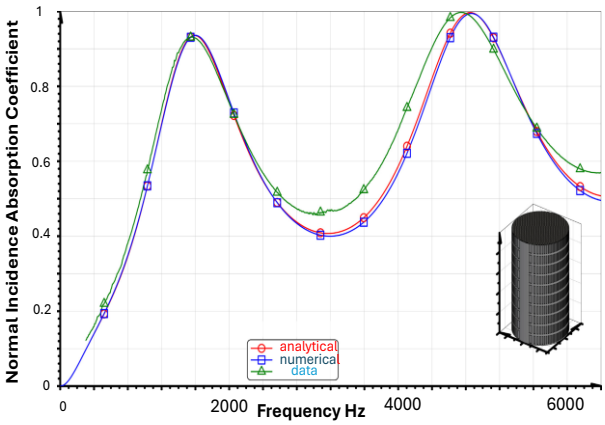

Figure 2 (Figure 8 from Ref.4) Measured normal incidence absorption spectrum and predictions for smooth walled identical slits obtained analytically and numerically using a Finite Element code.

Photographs of an edge and cross section of the cylindrical sample in Figs.3(a) and (b) show that the printed slit widths vary between 0.285 mm and 0.308 mm and the thickness of the separating walls varies between 0.401 and 0.436 mm. It is suggested that these variations and other internal surface imperfections may cause the discrepancies between predictions and data[4].

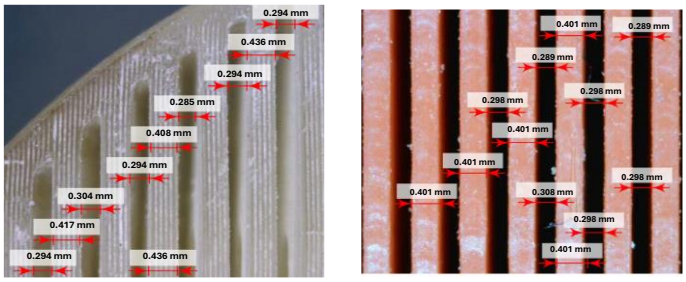

Figure 3. (from ref. 4 Figures 5(c) and (a)) Microscope images of the slits in 3D printed cylindrical samples showing variations in the widths of the slits and separating walls.

Figure 4 shows that the differences between predictions and data are reduced by assuming that the slit widths vary sinusoidally (eqns. (1) to (10) with $a = 0.03$ mm and $X = 0.248$ mm ($= d/200$)). The corresponding values of T_r and S are 1.076 and 1.325 respectively.

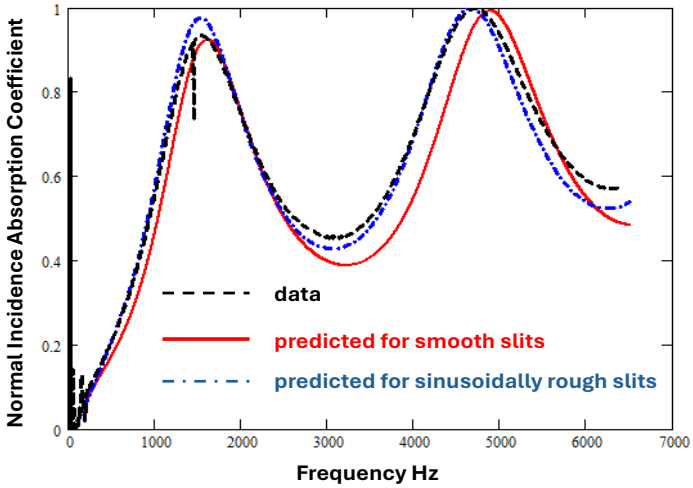

Figure 4 Comparison of measured[4] (broken black line) and predicted absorption spectra for a 3D printed sample containing vertical parallel slits with smooth (solid red line) or sinusoidal (dash-dot blue line) walls ($a = 0.03$ mm and $X = 0.248$ mm).

Figure 5 shows data and predictions for a sample containing zigzag slits with a fold length L_F = 1.25 mm (see inset in Fig.5)[4]. The grey line in Figure 5 is the prediction for infinitely long slits inclined at 45°. The 'analytical with folds' prediction makes use of an empirical tortuosity correction factor, C_F, to allow for the folds of length L_F in the zigzag slits given by[4]

$$C_F = \frac{4000L_F + (\cos\theta)^2}{4000L_F + 1}. \tag{11}$$

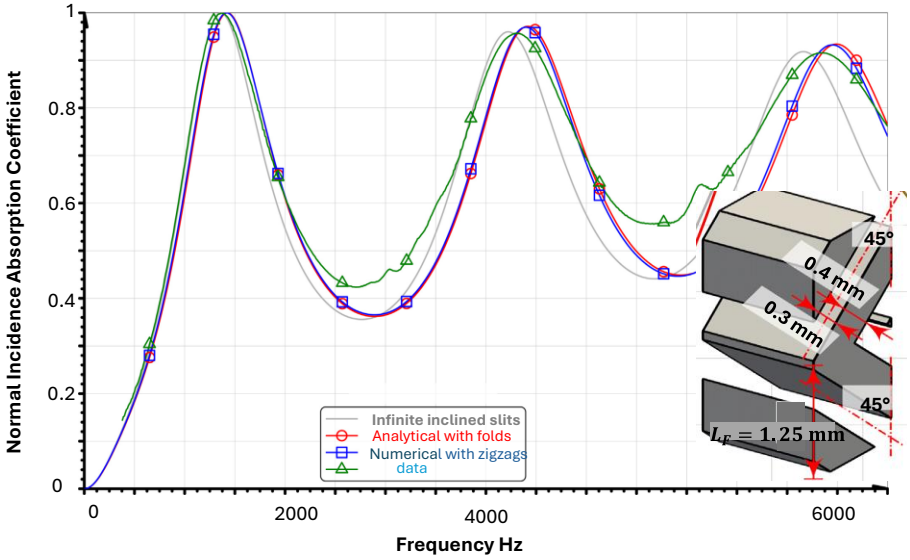

Figure 5 (based on Figures 11 and 12 in Ref.4) Measured normal incidence absorption spectrum (joined triangles) and analytical predictions for smooth walled identical infinitely long slits inclined at 45° (grey line), numerical predictions for zigzag slits using a Finite Element code (joined squares) and analytical predictions for slits (joined circles) including an empirical correction for the additional tortuosity associated with the zig-zag folds (equation (11) with L_F = 1.25 mm, $\theta = 45°$).

By including the empirical correction associated with the folds in the zigzags, the analytical prediction agrees well with the numerical prediction for zigzag slits, but neither of these predictions offer better agreement with the data than the prediction for infinitely long inclined slits. Figure 6 shows that agreement with the data can be improved by not only allowing for folds in the slits but also assuming that the slits have sinusoidally varying cross sections with $a = 0.025\ \mathrm{mm}$ and $X = 0.248\ \mathrm{mm}$. The corresponding values of C_F, T_r and S are 0.92, 1.053 and 1.24 respectively.

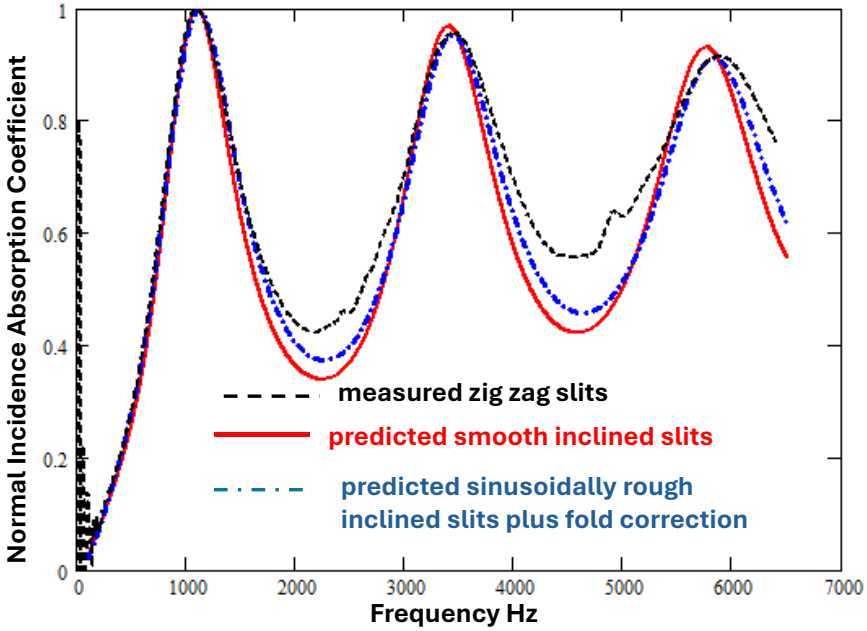

Figure 6. Comparison between the absorption spectrum measured on a 3D printed sample containing zigzag slits inclined at 45° to the surface normal (broken black line) and predictions for infinitely long slits either with parallel walls (solid red line) or folded and with sinusoidal walls ($a = 0.025\ \mathrm{mm}$, $X = 0.248\ \mathrm{mm}$, dash-dot blue line).

4 ABSORPTION BY WALNUT SHELLS AND WOOD CHIPS

Figure 7 shows cylindrical samples made from crushed walnut shells[7] and wood chips[8] together with Field Emission Scanning Electron Microscope (FE-SEM) images of representative constituent fragments showing their rough surfaces.

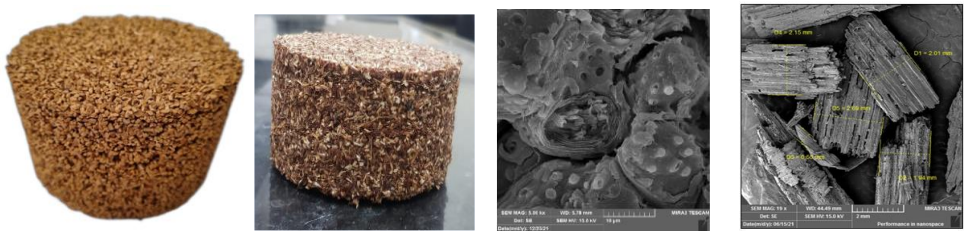

Figure 7. (left to right) cylindrical samples made from crushed walnut shells and wood chips, and FE-SEM images of walnut shell fragments (magnification 5000×) and wood chips (20×).

Figures 8 and 9 show data for the normal incidence absorption spectra of samples made from crushed walnut shells (20 mm and 40 mm thick) and wood chips (50 mm thick) respectively. Also shown are predictions for smooth and sinusoidal cross section slits using the independently (i.e. non-acoustically) measured values of porosity and flow resistivity listed in Table 1 and the values of slit semi width and sinusoidal cross section parameters listed in Table 2.

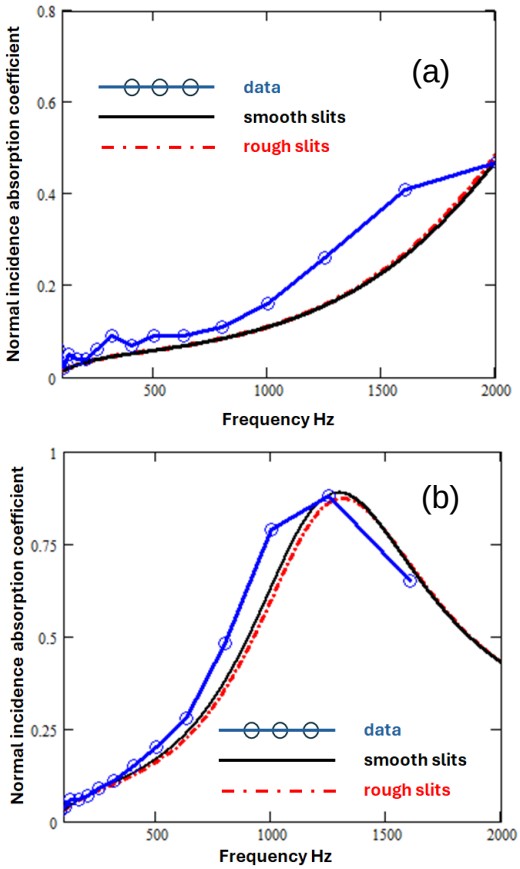

Figure 8. Measured normal incidence absorption of a) 20 mm and (b) 40 mm thick walnut shell samples[7] and predictions for inclined slits without (black continuous line) and with (red broken line) sinusoidal cross sections.

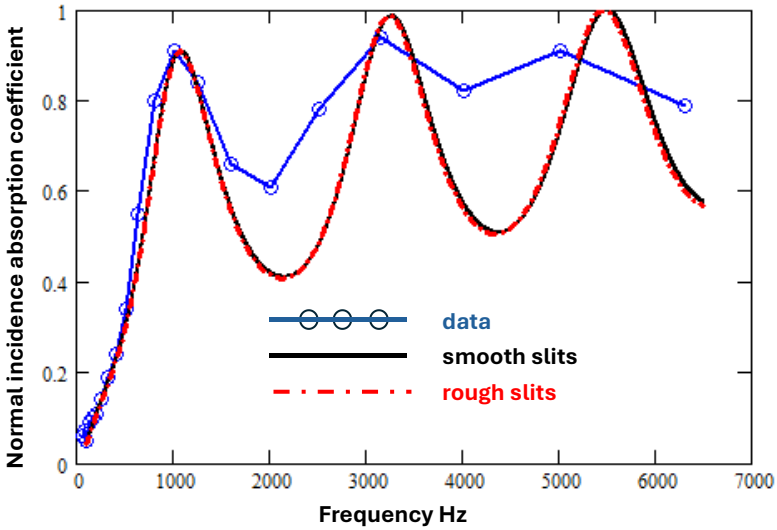

Figure 9. Measured normal incidence absorption spectrum of a 50 mm thick wood chip sample[8] (joined circles) and predictions for inclined slits without (continuous black line) and with (red dash-dot line) sinusoidal cross sections.

Some of the discrepancy between predictions and data in Figures 8 and 9 is caused by the data being in third octave bands whereas the predictions are at 50 Hz intervals.

Table 1. Measured porosity and flow resistivity of samples made from crushed walnut shell and wood chip and tortuosity fitted by assuming a pore structure of inclined identical slits.

sample	Porosity	Flow Resistivity Pa s m^{-2}	Tortuosity
walnut shell (20 mm)	0.619	5670	2.42
walnut shell (40 mm)	0.619	5405	2.42
Wood chip (50 mm)	0.684	5244	2.2

Table 2. Slit semi widths and sinusoidal roughness factors obtained by fitting data for crushed walnut shell and wood chip samples.

sample	smooth b mm	rough b mm	a mm	d mm	X mm	$T_r(a,d,N)$	$S(a,b,d,N)$
walnut shell	0.194	0.219	0.040	20	0.286	1.107	1.382
walnut shell	0.196	0.234	0.040	40	0.400	1.040	1.217
wood chip	0.183	0.220	0.045	50	0.250	1.129	1.453

The tortuosity values listed in Table 1 enable the prediction for identical slanted parallel sided slits to fit the first quarter wavelength resonance in the measured absorption spectrum. The slit width and sinusoidal cross section parameter values listed in Table 2 are those that result in the same values of flow resistivity and tortuosity (see Table 1) as parallel sided slits and thereby yield identical predictions of normal incidence absorption spectra. The values of the factors T_r and S in Table 2 indicate the influences of pore wall roughness on tortuosity and flow resistivity respectively for each of these examples. Since flow resistivity is inversely proportional to the square of slit semi width b, the predicted increases in flow resistivity and tortuosity due to sinusoidal pore walls imply that, to obtain the same values of tortuosity and flow resistivity, the mean values of b in the column headed 'rough b mm' are larger than those for parallel sided slits, in the column headed 'smooth b mm'.

5 INFLUENCE ON ABSORPTION OF SINUSOIDAL WALLS

Equations (1) to (10) can be used to investigate the extent to which the deliberate introduction of sinusoidal variations in slit width might improve the absorption of a low flow resistivity sound absorber containing vertical narrow slits. Figure 10(a) shows the influence on predicted normal incidence absorption coefficient spectra of varying the sinusoidal variation amplitude at constant wavelength and Figure 10(b) shows the influence of varying the wavelength at constant amplitude.

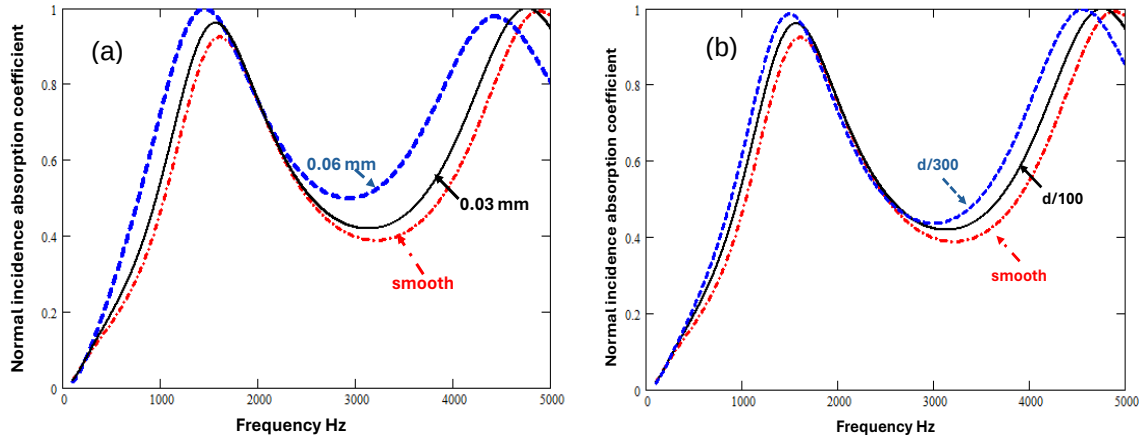

Figure 10. The predicted influence of sinusoidal slit parameters on normal incidence absorption coefficient of a 0.0495 m thick hard backed layer containing vertical slits of nominal width 0.3 mm (a) due to varying the amplitude of the sinusoidal variation in slit cross sections between 0 mm and 0.06 mm assuming a constant wavelength of 0.248 mm and (b) due to varying the wavelength between 0 mm and 0.165 mm assuming a constant amplitude of 0.04 mm.

Since they are predicted to cause increases in tortuosity and flow resistivity, either increasing the amplitude for a given wavelength or decreasing the wavelength for a given amplitude lowers the first quarter wavelength frequency and increases the absorption between quarter wavelength resonances. But, for a given wavelength, amplitude variation is predicted to have the greater influence.

6 CONCLUSIONS

A theory for the influence of a sinusoidal variation in slit pore cross section has been outlined and used to support the argument that the discrepancies between measured and predicted normal incidence absorption spectra for 3D printed samples with vertical and zigzag slits[4] are a consequence of the unevenness in the width of the slits.

Also, it has been used to estimate the influence of fragment surface roughness on the absorption measured for samples made from crushed nut shells and wood chips.

Furthermore, the extent to which the deliberate introduction of a sinusoidal variation in slit width can improve the absorption offered by a vertical smooth slit pore absorber has been investigated. For a given wavelength, the amplitude of the variation has a larger influence on the normal incidence absorption spectrum than variation in wavelength for given amplitude.

7 REFERENCES

1. K. Attenborough, Microstructures for lowering the quarter wavelength resonance frequency of a hard-backed rigid-porous layer, Applied Acoustics, **130** 188–194 (2018).
2. K. Attenborough, Macro- and Micro-structure designs for porous sound absorbers, Applied Acoustics, **145** 349–357 (2019).
3. K. Attenborough, Analytical Approximations for Sub Wavelength Sound Absorption by Porous Layers with Labyrinthine Slit Perforations. Applied Science, **11** 3299 (2021).
4. K. C. Opiela, T. Zielinski and K. Attenborough, Limitations on validating slitted sound absorber designs through budget additive manufacturing, J. Materials and Design, 110703, (2022).
5. Song SY, Yang XH, Xin FX, Ren SW, Lu TJ. Modeling of roughness effects on acoustic properties of micro-slits. J Appl Phys D. **50** 235303 (2017).
6. M. R. Stinson, The propagation of plane sound waves in narrow and wide circular tubes, and generalization to uniform tubes of arbitrary cross-sectional shape. The Journal of the Acoustical Society of America, **89** 550-558 (1991).
7. K. Attenborough, M. J. SheikhMozafari, E. Taban, L. Tajik, S. Rasaneh and M. Faridan, Sound Absorbers from Waste Walnut Shells, Proc. InterNoise 2024, Nantes, France
8. M. Lashgari, E. Taban, M. Javad SheikhMozafari, P. Soltani, K. Attenborough, A. Khavanin, Wood Chip Sound Absorbers: Measurements and Models, Applied Acoustics **220** 109963 (2024).